POST PRINT

https://www.sciencedirect.com/science/article/pii/S088723331730036X?via%3Dihub

https://doi.org/10.1016/j.tiv.2017.02.014, Toxicology in Vitro 41 (2017) 64–74

Glucose capped silver nanoparticles induce cell cycle arrest in HeLa cells

Elisa Panzarini[1], Stefania Mariano[1], Cristian Vergallo[1], Elisabetta Carata[1], Gian Maria Fimia[1], Francesco Mura[2], Marco Rossi[2], Viviana Vergaro[1], Giuseppe Ciccarella[1,3], Marco Corazzari[4], Luciana Dini[1,3]

[1]Department of Biological and Environmental Sciences and Technologies (Di.S.Te.B.A.), University of Salento, Lecce, Italy; [2]Department of Base and Applied Science to Engineering Sapienza University of Rome, Rome, Italy; [3]CNR Nanotec, Lecce, Italy; [4]Department of Biology, University of Rome Tor Vergata, Rome, Italy

Corresponding Author:
Luciana Dini
University of Salento, Department of Biological and Environmental Sciences and Technologies (Di.S.Te.B.A.), Comparative Anatomy and Cytology Laboratory, Centro Ecotekne, Via Prov.le Lecce-Monteroni, 73100 Lecce. Tel: +390832298614; Fax: +390832298937; email: luciana.dini@unisalento.it

Authors email: elisa.panzarini@unisalento.it; stefania.mariano@unisalento.it; cristian.vergallo@unisalento.it; elisabetta.carata@unisalento.it; gianmaria.fimia@unisalento.it; francesco.mura@uniroma1; marco.rossi@uniroma1.it; marco.corazzari@uniroma2.it; luciana.dini@unisalento.it

Abstract

This study aims to determine the interaction (uptake and biological effects on cell viability and cell cycle progression) of glucose capped silver NanoParticles (AgNPs-G) on human epithelioid cervix carcinoma (HeLa) cells, in relation to amount, $2x10^3$ or $2x10^4$ NPs/cell, and exposure time, up to 48 h.

The spherical and well dispersed AgNPs (30 ± 5 nm) were obtained by using glucose as reducing agent in a green synthesis method that ensures to stabilize AgNPs avoiding cytotoxic soluble silver ions Ag^+ release. HeLa cells take up abundantly and rapidly AgNPs-G resulting toxic to cells in amount and incubation time dependent manner. HeLa cells were arrested at S and G2/M phases of the cell cycle and subG1 population increased when incubated with $2x10^4$ AgNPs-G/cell. Mitotic index decreased accordingly. The dissolution experiments demonstrated that the observed effects were due only to AgNPs-G since glucose capping prevents Ag^+ release.

The AgNPs-G influence on HeLa cells viability and cell cycle progression suggest that AgNPs-G, alone or in combination with chemotherapeutics, may be exploited for the development of novel antiproliferative treatment in cancer therapy. However, the possible influence of the cell cycle on cellular uptake of AgNPs-G and the mechanism of AgNPs entry in cells need further investigation.

Keywords: silver nanoparticles (AgNPs); cytotoxicity; cell cycle; nanoparticles uptake; HeLa cells

Background

Nowadays, the research about NanoMaterials is continuously expanding because they possess novel physical and chemical functional properties exploitable in the manufacture of devices with unique properties (Colvin, 2003). In particular, the use of NMs on pharmaceutical industry is undergoing development at an increasing fast rate (Etheridge et al., 2013). NMs are applied in medical sector mainly as imaging sensors and drug delivery carriers since they are capable to pass biological barriers and enter and distribute within cells (Etheridge et al., 2013). A variety of functional NMs (such as quantum dots, nanotubes, polymeric and magnetic nanoparticles) are ongoing in many clinical trials evaluation (Bourzac, 2012).

Among all the NMs used in consumer products, silver NanoParticles (AgNPs) have currently the highest degree of commercialization in manufacturing deodorants, clothing, bandages, cleaning solutions, sprays and medical products (Woodrow, 2011), due to the antimicrobial properties of the silver (Chen and Schluesener, 2008).

The major toxicological concerns in the use of AgNPs depend on the possible release of Ag^+ ions upon interaction with cells (Park et al., 2010) that can be prevented by coating AgNPs with several types of molecules, (e.g., citrate, chitosan, polysaccharides, glycans, starch). These molecules promote NPs stability, prevent agglomeration and improve AgNPs biocompatibility too (Ahamed et al., 2008).

To assess the nanosafety of NPs, different aspects have to be taken into consideration. In the case of AgNPs in consumer products, normal cells are a good model for testing the biosafety for animal or human cells (Beer et al., 2012). When a possible application in cancer therapy is taken into consideration, the use of tumor cells is needed (Arora et al., 2008). Very recently, AgNPs have been exploited in high sensitivity biomolecular detection, diagnostics and therapeutics as the main application in human health. In addition, AgNPs are also receiving significant attention in cancer management, being a suitable theranostic agents (Sharma et al., 2015). Interestingly, the optical

properties of AgNPs make them a potent candidate as photosensitizer in photodynamic treatment, a cancer therapy based on application of light (El-Hussein et al., 2015).

The safe use of AgNPs needs that the entire process, from synthesis to characterization, have to be investigated. In fact, the importance of the method used to synthetize of AgNPs was emphasized many times. The impact of NPs on cells strictly depends on their cellular uptake that, in turn, relies on many factors, including NPs composition, size, shape, and coating (Cho et al., 2010; Albanese et al., 2012). AgNPs cause toxic responses *via* induction of oxidative stress as consequence of the generation of intracellular reactive oxygen species (ROS), depletion of glutathione (GSH), reduction of the superoxide dismutase (SOD) enzyme activity, and increased lipid peroxidation (Arora et al., 2008; Hussain et al., 2005; Dini et al., 2011; Vergallo et al., 2014; Panzarini et al., 2015). Moreover, AgNPs interfere with cell cycle as reported in various *in vitro* cell models (Park et al., 2010; Asharani et al., 2009; Wei et al., 2010; Liu and Hart, 2010; Eom and Choi, 2010; Piao et al., 2011). A role in the uptake of NPs has been recently attributed to the cell cycle. Kim et al. (2011) reported that internalized amount of NPs varies as cell advances through the cell cycle.

We have recently demonstrated that the different glycans-capped AgNPs (glucose, glucose/fructose and glucose/sucrose) influence the cellular responses in terms of viability, induction of different cell death types, ROS generation and lipid peroxidation in HeLa and HepG2 cells, and in human lymphocytes, in which AgNPs-G absorption/internalization was also shown (Dini et al., 2011; Vergallo et al., 2014, 2016; Panzarini et al., 2015). Indeed, modulation of toxicity and uptake of AgNPs by carbohydrate functionalization has been reported (Kennedy et al., 2014). The aim of this study deals with the analysis of the interaction (uptake and biological effects) of 30 nm AgNPs with Human epithelioid cervix carcinoma (HeLa) cells. Two different doses ($2x10^3$ or $2x10^4$ NPs/cell corresponding to 1,35µg/mL and 13,5µg/mL of $AgNO_3$ dissolved in the culture medium) of β-D-Glucose-coated silver NanoParticles (AgNPs-G) were used. To rule out the contribution of eventually released Ag^+ to the toxicity of AgNPs-G, a preliminary evaluation of the level of NPs dissolution in culture medium was done. HeLa cells response to AgNPs was analyzed by using

Graphite Furnace-Atomic Absorption Spectrometry (GF-AAS), Inductively coupled plasmon optical emission spectroscopy (ICP-OES), Scaning Electron Microscopy-Energy Dispersive X-ray (SEM-EDX) and Fluorescence Activated Cell Sorting (FACS).

Methods

Chemicals.

All chemicals were of analytical grade and were purchased from Sigma-Aldrich (Sigma, St. Louis, MO, USA) unless otherwise indicated.

AgNPs-G synthesis, characterization and stability

AgNPs-G were obtained by adding 2 mL of a 10^{-2} M aqueous solution of $AgNO_3$ to 100 mL of 0,3 M β-D-Glucose water solution. The mixture was boiled for 30 minutes under vigorous stirring. Yellow colour of the solution indicated the formation of AgNPs. Deionized ultra-filtered 18.2 MΩ water prepared with a Milli-Q Integral Water Purification System (Merck Millipore Headquarters, Billerica, MA, USA) was used for all experiments. All glassware were washed in ultrasonic bath of deionized water and not ionic detergent, followed by thorough rinsing with Milli-Q water and ethanol (Carlo Erba, Milan, Italy) to completely remove not ionic detergent contaminants. Finally glassware were dried prior to use.

The average and distribution size, morphology and stability of the NPs have been studied by high resolution TEM and UV-visible spectroscopic techniques.

Transmission Electron Microscopy (TEM) observations were performed by a Hitachi 7700, at 100 kV (Hitachi High Technologies America Inc., Dallas, TX, USA). The specimens were prepared for TEM observations by placing small droplets of AgNPs-G solutions onto standard carbon supported 600-mesh copper grid and air dried. Particles size distribution has been obtained using the ImageJ program (US NIH, Bethesda, USA). A histogram was created for 500 counted particles. Selected area electron diffraction (SAED) patterns were also obtained.

UltraViolet-Visible (UV-Vis) spectra were recorded in the range between 300 and 800 nm by using a T80 spectrophotometer (PG Instruments Ltd, Leicester, UK). Optical spectra were obtained by

measuring the absorption of the solution in a quartz cuvette with a 1 cm optical path. The stability of different AgNPs-G concentrations was assayed in EMEM culture medium up to 10 days.

The dissolution of AgNPs-G, in terms of release of Ag^+, up to 10 days in EMEM culture medium was determined by atomic absorption spectroscopy (AAS; Thermo Electron Corporation, M-Series) after precipitation of AgNPs-G by ultracentrifugation (24,900 g; 30 min at 4°C). The detection limit was 1 µg/L. Triplicate readings were analyzed for each point and control samples of known Ag concentration were analyzed in parallel generating data with the standard deviation of three independent samples. Results were expressed as the mean amount of Ag in µg/mL. Silver ions dissolution degree was expressed as percentage (%) of total Ag^+, as $AgNO_3$, added to reach the concentration of NPs during treatment.

The stability of capping of glucose was evaluated by sugar quantification up to 10 days in EMEM complete culture medium *via* spectrophotometric Glucose assay kit ab65333 (abcam, Cambridge, UK).

Cell culture and treatment conditions.

Human epithelioid cervix carcinoma HeLa cells were cultured in Eagle′s Minimum Essential Medium (EMEM) (Cambrex, Verviers, Belgium) supplemented with 10% fetal calf serum (FCS), 2 mM L-glutamine (Cambrex, Verviers, Belgium), 100 IU/ml penicillin and streptomycin solution and 10000 U/ml nystatin (antimicotic solution) (Cambrex, Verviers, Belgium), in a 5% CO_2 humidified atmosphere at 37°C. Cells were maintained in 75 cm^2 flasks (concentration ranged between $2x10^5$ and $1x10^6$ cells/mL) by passage every 3 to 4 days. HeLa cells were seeded for each sample and used 24 h after the attachment to substrate, which was considered as time 0 (T0). The cells were treated for 15 and 30 minutes, 1, 3, 6, 12, 18 and 24 h with $2x10^3$ or $2x10^4$AgNPs-G/cell. The amounts of NPs chosen, *i.e.*, $2x10^3$ and $2x10^4$ AgNPs/cell corresponding to 1,35µg/mL and 13,5µg/mL of $AgNO_3$, are the less and the more toxic for HeLa cells respectively, as previously reported (Dini et al., 2011). The toxicity of Ag^+ or β-D Glucose was evaluated. Incubation with EMEM culture medium alone was used as negative control.

MTT viability assay

At fixed times after AgNPs-G exposure, the culture medium was discharged, the cells were washed two times with Phosphate-Buffered Saline (PBS) 0,2 M pH 7,4 and fresh culture medium containing 1 mg/mL of 3-(4,5-dimethylthiazol-2-yl)-2,5-diphenyltetrazolium bromide salt (MTT) was added to each well. After 2 h of incubation at 37°C in a 5% CO_2 humidified atmosphere, MTT was reduced to formazan salt, a dark insoluble product, by the mitochondrial reductase of vital cells. Then, formazan salts were dissolved in DiMethylSulfOxide (DMSO), leading to a violet solution whose absorbance was measured with Ultrospec 4000 UV-visible spectrophotometer (Pharmacia Biotech, Stockholm, Sweden) at 570 nm. Viability was expressed as percentage of the Relative Growth Rate (RGR) by the equation:

$$RGR = (D_{sample}/D_{control}) \times 100$$

where D_{sample} and $D_{control}$ are the absorbance of the test samples and the negative controls, respectively.

Membrane integrity: LDH measurement

Cell membrane integrity of HeLa cells was evaluated by determining the activity of lactate dehydrogenase (LDH) leaking out of the cell according to the manufacturer's instructions (Lactate Dehydrogenase Activity Assay Kit, Sigma-Aldrich, St. Louis, USA). The LDH assay is based on the release of the cytosolic enzyme, LDH, from cells with damaged cellular membranes. Thus, in cell culture, the course of AgNPs-G induced cytotoxicity was followed quantitatively by measuring the activity of LDH in the supernatant. Cells were exposed to fixed AgNPs-G concentrations for 15 and 30 minutes, 1, 3, 6, 12, 18 and 24 h, then 50 µL per well of each cell-free supernatant was transferred into wells in a 96-well, and 50 µL of LDH assay reaction mixture was added to each well. After 3 hours of incubation under standard conditions, the optical density of the color generated was determined at a wavelength of 450 nm by using Thermo electron corporation MULTISKAN EX ORIGINAL (Thermo Fisher Scientific Inc., Waltham, MA, USA).

Cell cycle analysis

For cell cycle analysis, HeLa cells were incubated with AgNPs-G ($2x10^3$ or $2x10^4$AgNPs-G/cell) as reported in the section entitled ”Cell culture and treatment conditions”. At each time point, cells at the concentration of $2x10^6$ cells/mL were washed with PBS (0.2 M, pH 7.4), detached with trypsin and fixed in cold ice methanol/aceton (4:1). Subsequently, the cells were stained with Propidium Iodide (PI) containing RNase (60 µg/mL and 100 µg/mL in PBS, respectively) and analyzed using a FACScan BD (Becton Dickinson Biosciences, New Jersey, USA). The percentage of cells in the sub-G1 phase of the cell cycle was calculated from the total 10,000 cells (100%) in the assay, and that for cells in G0/G1, S and G2/M phases was calculated from the total cells excluding the sub-G1 cells.

Immunocytochemical Analysis

For immunocytochemistry, $15x10^4$ HeLa cells were grown on glass coverslips for 24 h before incubation with AgNPs-G ($2x10^3$ or $2x10^4$ NPs/cell) or β-D-glucose solution (4,6 mM and 46 mM) for 24 and 48 h. Cells were fixed with formalin (4% in PBS 0.2 M, pH 7.4) and then incubated with blocking solution (3% bovine serum albumin in PBS 0.2 M, pH 7.4) for 15 minutes at room temperature and permeabilized for 1 minute with methanol at -20°C. Samples were incubated 1 h at room temperature with 1 µg/mL anti-phospho Histone H3(Ser 10) Mitosis Marker antibody (Millipore, Billerica, MA, USA), followed by 1 h incubation with 1 µg/mL FITC-conjugated anti-rabbit IgG at room temperature in the dark. Slides were mounted and observed with fluorescence microscopy Eclipse 80i (Nikon, Tokyo, Japan), using a band-pass filter (excitation 490 nm, emission 520 nm). At least 500 cells were scored. Mitotic Index (MI) was calculated by the equation:

$$MI = (labeled\ cells/total\ cells) \times 100$$

where *labeled cells* and *total cells* are the number of all mitotic figures, *i.e.* prophase, metaphase, anaphase, and telophase, and total counted cells (taken as 100%), respectively.

Cell uptake of AgNPs-G

A Graphite Furnace Atomic Absorption Spectrometry (GF-AAS), by using a spectrometer Varian Spectral-600 (Varian Inc., Palo Alto, USA), was used for silver quantitative analysis. It was equipped with a silver hollow cathode lamp and an autosampler Varian GTA 100, powered by high-purity argon as inert gas and water for the cooling process. A Zeeman effect was exploited in order to eliminate the background absorption. The amounts of AgNPs-G internalized into the HeLa cells were indirectly measured as the decrease of silver concentration (ppm) in the culture medium at fixed intervals of time after AgNPs-G administration to cells.

Inductively coupled plasmon optical emission spectroscopy (ICP-OES)

HeLa cells were incubated with AgNPs-G ($2x10^3$ or $2x10^4$AgNPs-G/cell) for 30 minutes, 2 and 4h as reported in the section entitled "Cell culture and treatment conditions". After harvesting, the culture medium was collected and centrifuged (5 minutes, 1000 rpm, 4°C) to remove cell debris. The supernatant was frozen (24h at -20°C), lyophilized and stored at –80°C until analysis. The cells were washed twice with PBS to remove potential medium residue, detached from substrate and centrifuged. The supernatants were discarded and the cell pellets were extracted in 2 mL perchloric acid (PCA, 0.9 mol/l). The samples were sonicated (Brooklyn Instruments, NY, USA) for 60 s and then centrifuged for 15 min (1000 rpm at 4°C). The supernatant pH values were then adjusted to 7.0±0.1 using 1 mol/l KOH and 1 mol/l HCl, followed by centrifugation (3000 g at 4°C) for 10 min. The resulting clear supernatants were lyophilized and stored at –80°C until analysis. Before the ICP-OES analysis (Perkin Elmer Optima 7300 V HF version, MA, USA) the samples were neutralized in concentrated HNO_3 for 5 min on a heating block. The measurements were performed against silver standard of 1 mg/L. The results are reported as ratio of Ag^+ in cell extract/ Ag^+ in cell culture.

SEM-EDX analysis

Scanning Electron Microscopy-Energy Dispersive X-ray (SEM-EDX) analysis was used to identify AgNPs-G within HeLa cells. HeLa cells were incubated for 30 minutes and 2 h with AgNPs-G ($2x10^3$ or $2x10^4$ NPs/cell) and embedded in Agar solution (5% in water). The cells were dehydrated

in increasing ethanol concentration and embedded in 54°C paraffin (BIO-OPTICA Strumentazioni Scientifiche, Milano, Italy). Five micrometer-thick sections were cut by using a microtome Reichert-Jung 2050 Supercut (Leica Microsystems GmbH, Wetzlar, Germany) and placed on steel stub and air dried. EDS measurement were performed on a EDX Bruker Quantax (Bruker Nano, New Jersey, USA) incorporated into a Fesem Zeiss Auriga 405 (Zeiss, Oberkochen, Germany).

Statistical Analysis

The results are reported as mean ± standard deviation (SD) of 3 technical replicates in each of the 3 independent experiments. To test differences between the control (untreated cells) and AgNPs-G ($2x10^3$ NPs/mL or $2x10^4$ NPs/mL) groups a Two-Way ANOVA was used. Additionally, independent samples with equal variances were assessed for statistical significance with a *t*-test. P values < 0.05 were considered to be statistically significant.

Results

AgNPs characterization

Morphology, size (average and distribution), and stability of the AgNPs-G freshly prepared and after 10 days in EMEM cell culture medium are shown by TEM micrographs, diffraction pattern, particle size distribution and UV-visible spectra of AgNPs-G as reported in Figures 1 and 2. The UV-visible absorbance spectra of freshly synthesized AgNPs-G (Fig. 1a) shows a strong extinction band with a maximum at 420 nm, characteristic absorption wavelength of spheroidal AgNPs. A significant change/shift of the extinction band and a dramatic decrease in the absorbance intensity after 10 days in EMEM is evident. In fact a second peak at 600-700 nm was observed (Fig. 1a). The diffraction patterns of freshly synthesized AgNPs show the nanocrystalline nature of NPs (Fig. 1b). After 10 days in EMEM medium the ring structure of SAED pattern shows evident bright spots, that indicate the change in crystalline structure, confirming the loss of stability of AgNPs solution (Fig. 1b). AgNPs-G are mostly spherical and well-dispersed in freshly prepared solution (Fig. 2a). The size distribution ranges from 20 to 40 nm and the average size is d = 30 nm with a standard

deviation of 5 nm. After 10 days in culture medium, a significant difference in shape and size of AgNPs-G compared with freshly synthetized NPs was observed: an increasingly number of nanorods are observed (average longitudinal diameter = 50 nm; standard deviation = 25 nm) (Fig. 2b).

It is known that particle toxicity could depend on Ag^+ released from NPs, thus the stability of AgNPs in the culture medium was estimated. Using the atomic absorption spectroscopy, free Ag^+ was determined in complete EMEM culture medium up to 10 days (Table 1). AgNPs-G were stable in culture medium up to 10 days. In fact, the dissolution degree, expressed as percentage of total Ag^+ ranges between 1,98 and 5,72% at 1 and 10 days respectively (Supplementary figure 1). The maximum amounts of Ag^+ released at 10 days are 0,077 and 0,772 µg/mL corresponding to dissolution of $2x10^3$ and $2x10^4$ AgNPs/cell solutions respectively. These amounts were used to assess HeLa cell viability as below described. The capping of glucose is stable up to 10 days since during the immersion tests, the glucose in culture medium did not increase (data not shown).

Effect of AgNPs-G on cell viability

Time course of HeLa cells viability incubated with different amounts of AgNPs-G was assessed by MTT and LDH assay (Fig. 3). The reduced viability of HeLa cells in the presence of AgNPs-G was concentration- and incubation time-dependent. In general, the highest amount of AgNPs-G ($2x10^4$ NPs/cell) was more toxic than lowest one ($2x10^3$ NPs/cell) at any time of incubation. At 12h of incubation (reduction of about 45% and 75% *vs* untreated HeLa cells in the presence of $2x10^3$ NPs/cell and $2x10^4$ NPs/cell, respectively) was found the maximum of toxicity. Interestingly, cells incubated with the lowest amount of NPs for 24 and 48 h expressed viability comparable to untreated cells one (Fig. 3A). To further analyze the effect of AgNPs-G on HeLa cells viability, plasma membrane integrity was assayed. LDH assay data corroborate MTT findings: significant LDH levels increase with the highest amount of AgNPs-G and maximum of toxicity was seen at 12h. The results show that HeLa cells membrane integrity compromision was AgNPs-G dose- and incubation time-dependent (Fig. 3B).

Cell morphology changed accordingly to the decrement of HeLa cell viability (Fig. 3C). Features of cell toxicity (cell shrinkage, detachment from bottom of flask, floating cells, blebbing) were observed. To rule out the contribution of the β-D-glucose and Ag^+ to toxicity of AgNPs-G, cells were incubated with either β-D-glucose or $AgNO_3$ alone. β-D-glucose concentrations were equivalent to those present in the AgNPs solutions, while Ag^+ concentrations were equivalent to the maximum concentrations of Ag^+ dissolute from AgNPs at 10 days (Table 1). Neither β-D-glucose nor Ag^+ exert a noticeable influence on cell viability in the concentrations considered, confirming that cytotoxicity only depends on AgNPs (Fig. 3A and 3B).

Uptake of AgNPs-G.

The ability of HeLa cells to uptake AgNPs-G was investigated by using GF-AAS, ICP-OES and SEM-EDX analysis (Fig. 4). GF-AAS determines the concentration of free chemical elements of a solution; thus the silver concentration in the HeLa cells culture medium is the indirect indication of the AgNPs uptake. ICP-OES is a technique commonly used for the analysis of metals in various fields based on Atomic Emission Spectroscopy, where the sample at high temperature plasma up to 8000 Kelvin is converted to free, excited or ionized ions. The ions emit a radiation when go back to ground state, whose intensities are optically measured and indicate the amount of ions. SEM-EDX allows the elemental analysis or chemical characterization of a sample coupled with the direct visualization of NPs inside the cells. Comparable results were obtained with the different techniques (Fig. 4).

The amount and the kinetic of AgNPs uptake are shown in Figure 4A. The AgNPs-G uptake, expressed as ppm of silver, depends on NPs amount and incubation time. In fact, a consistent NPs cellular uptake was only observed for $2x10^4$ AgNPs-G/cell incubation, whereas a very low NPs internalization was found with $2x10^3$ AgNPs-G/cell. Internalization was very low for the first 30 minutes of incubation with NPs when rapidly decreased, reaching the peak in about the next hour. The NPs amount internalized remained constant in between 2 and 3 h of incubation, to rapidly decrease and to be almost negligible in about 12 h. Thus, the interval time in which HeLa cells were

actively taking up AgNPs-G is from 1 to 3 hrs, indicating that internalization was quite an early event.

ICP-OES allows to evaluate for each time point the silver ions in culture medium and in cell extracts, giving an indirect quantification of internalized AgNPs. Data reported in Figure 4B confirm that internalization is rapid (from 30 minutes to 2h of incubation) and efficiency depends on NPs amount ($2x10^4$ NPs/cell more than $2x10^3$ NPs/cell) and incubation time (peak of internalized NPs at 2h). The Ag^+ present in the cell extract was 2 and 5 folds higher than those in the culture medium at 30 minutes and 2h of treatment, respectively. The progressively reduced internalization observed by GF-AAS analysis from 6h, is confirmed by the peak of silver in the culture medium (0,3 folds *vs* cell extract) measured at 18h of incubation with the highest dose of NPs (Fig. 4B).

In Figure 4C, EDX spectrum of the red squared area in the SEM micrograph showing white brilliant spots in the middle of the cell obtained at approximately 3 keV, displays the silver peak. Conversely, the peak was absent in the spectra obtained considering the cellular area outside the white brilliant spots. It is worth noting that AgNPs-G, once inside the cell, moved rapidly to more internal cytoplasmatic localization where they are found as aggregates. Simultaneously, other AgNPs-G are taken up by the cell and can be seen, not yet aggregated, as small brilliant white spots localized at the cell periphery.

Effect of AgNPs on the cell cycle.

All phases of the cell cycle, *i.e.*, DNA synthesis (S), gap2/mitosis (G2/M), gap1 (G0/G1) and sub-G1 (includind dead cells and cellular debris), were analyzed (Fig. 5 and 6). In general, the presence of $2x10^4$AgNPs-G/cell influenced the entire cell cycle and in particular the G2/M phase. We found an arrest in G2/M phase of HeLa cells at 6 h up to 24 h. 50% and 60% of HeLa cells incubated with AgNPs-G more than unexposed ones were in G2/M phase at 6 h (Fig. 5A) and 24 h (Fig. 5D), respectively. A consistent block of cells in S phase at 12 (about 20% more than untreated cells) (Fig. 5B) and 18 h (about 50% more than untreated cells) (Fig. 5C) were found. Conversely, the

cells number in S phase significantly decreases of about 30% *vs* unexposed HeLa cells at 6 h of culture (Fig. 5A). A significant decrement of quiescent/growing cells (G0/G1 phase) was observed from 12 h to 24 h of treatment, reaching the peak of 25% less than untreated cells at 18h (Fig. 5C). In Supplementary figure 2 we report flow cytograms of results plotted in Figure 5.

The significant increment of the sub-G1 population in a AgNPs-G amount- and incubation time-dependent manner confirms the toxicity of AgNPs-G (Fig. 6). A significant high percentage of sub-G1 cells was already seen soon after 30 minutes of incubation with the highest amount of AgNPs-G that at 18h were about 30% of cell population; thus, the maximum increment in sub-G1 was of 95% *vs* untreated cells at 18h (Fig. 6).

The influence of AgNPs-G on cell cycle was further investigated by evaluating the Mitotic Index (MI) of HeLa cells cultured for 24 and 48 h in the presence of AgNPs-G, by using the specific marker for cells undergoing mitosis, Phospho-histone H3 (PHH3) (Goto et al., 1999). MI of HeLa cells incubated with $2x10^3$ or $2x10^4$ AgNPs-G/cell for 24 and 48 h are reported in Figure 7 and represent the counts of all mitotic figures, *i.e.* prophase, metaphase, anaphase, and telophase. MI was affected only the highest AgNPs-G amount (85 and 95% with respect to untreated cells at 24 and 48 h respectively). β-D-glucose did not influence MI of HeLa cells.

Discussion

In the present work we demonstrated that AgNPs-G, synthesized by green chemistry using β-D-glucose as reducing agent, enter HeLa cells and exhibit strong toxicity. In our experiments, NPs in an amount- and incubation time- dependent manner decrease cell viability and perturb cell cycle. Since β-D-glucose capping ensures very low dissolution of Ag^+ from AgNPs and no loss of glucose was observed, the toxicity is due only to NPs. Our choice to exploit β-D-glucose during the synthesis of AgNPs is based on the literature data reporting that among surface coatings there is an increasing interest in using carbohydrates as functional molecules on the surface of nanoparticles (Kennedy et al., 2014; Marradi et al., 2013; Chiodo et al., 2014). In fact, glycans offer several advantages: (a) allow that synthesis can be performed under biomimetic conditions that produce

NPs without traces of harmful chemicals responsible for adverse cellular responses (Loza et al., 2014); (b) can serve as targeting molecules, e.g. for the diagnosis and treatment of brain diseases (Zhang et al., 2014; Farr et al., 2014); (c) stabilize and ensure NPs dispersity. In addition, we have already observed that the type of glycan hardly affects the degree of biocompatibility of AgNPs (Dini et al., 2011; Panzarini et al., 2015). The experimental design, in terms of amounts of AgNPs used and time of treatment, is based on previous results. Also, the cell type considered, *i.e.*, HeLa cell line, has tremendous importance in biomedical research since HeLa cells were disseminated around the world and became the basis for numerous medical studies that have benefited humankind.

To induce biological effects NPs must be attached to or enter into and distribute within cells (Sahay et al., 2010). AgNPs-G internalization by HeLa cells appears to be an early and fast event after the addition of AgNPs-G to the culture medium and lasts only few hours, *i.e.*, 2-3 h. Interestingly, few NPs were captured by HeLa cells when the culture medium NPs amount is low; conversely, the presence of a reliable number of NPs induced HeLa cells to a consistent internalization. This data, that are in contrast with a previous study in which by using peripheral human lymphocytes we measured a conspicuous uptake of both low and high amount of NPs (Vergallo et al., 2014), suggest that not only the NPs characteristics influence the interactions with cells but also the cell type.

The kinetic uptake experiments showed that internalization process has a limited duration and was completed in about 2-3 hours. This can be due to the onset of cell death as shown by the progressive increase of the subG1 peak, that, in turn, limits the number of cells that can actively interact with the NPs.

As well reviewed by Kim (2013), AgNPs induce many signs of toxicity, like oxidative stress, genotoxicity and apoptosis, which could be associated to Ag^+ release and/or agglomeration/aggregation of AgNPs. For example, the particular microenvironment of cancer, may transform nanosilver into ionic form under influence of certain chemical mediators, like ROS. In addition, even when the AgNPs pass through the cell membrane and enter the cells, additional Ag^+

may be created and express cytotoxic or genotoxic effects. Other source of toxicity can derive by the chemical compounds used during the synthesis. Finally, also the nature of immersion medium is an important factor influencing NPs dissolution (Loza et al., 2014). Thus, new safe synthesis techniques are developing to avoid these concerns. To properly explore the mechanisms of toxicity of AgNPs, it is important to rule out if it is caused by Ag^+. In this study, we used AgNPs-G produced by the so-called *green chemistry*, a method to overcome the shortcomings of current chemical AgNPs synthetic routes. This procedure does not use toxic compounds during synthesis and prevents the release of Ag^+ in culture medium in two manners. First, NPs never underwent sonication, that potentially promotes the dissolution of AgNPs into Ag^+ by increasing thermal energy able to break bigger AgNPs aggregates (Liu and Hart, 2010), or any other method of artificial decrease of particle size. In addition, β-D-glucose coating prevents AgNPs oxidation, which causes release of Ag^+, and ensures both stability and dispersity of AgNPs in culture medium (Dini et al., 2011). In fact, the characterization analysis in culture medium up to 10 days suggested that the solution of AgNPs-G used in all the experiments is stable for at least 48h, corresponding to the duration of the treatment performed. Also, the biological effects described only depend on NPs and not on the release of Ag^+ or on the saccharides used during NPs preparation, in accord with our previous work (Dini et al., 2011; Vergallo et al., 2014, 2016; Panzarini et al., 2015). Residual Ag^+ derived from AgNPs are present in very low amount in the culture medium during the experiments as indicated by the percentage of dissolution (between 2 and 5% up to 10 days of immersion) of AgNPs in complete EMEM culture medium under culture conditions, 37°C and 5% CO_2. The amount of Ag^+, detected by spectroscopic analysis, is very low during the experiment and does not affect cell viability suggesting that the biological effects of AgNPs-G only depend of silver in nanoform. It is worth noting to mention that also glucose capping was very stable up to 10 days in culture conditions, independently of the amount of NPs/cell. Cytotoxicity of AgNPs depends on amount and duration of cell treatment. This data are in agreement with our previous work, in which the less ($2x10^3$) and the more ($2x10^4$) toxic AgNPs amounts for HeLa cells and time of treatment

were determined (Dini et al., 2011; Panzarini et al., 2015). In particular, under non-cytotoxic exposure conditions of AgNPs (low amount of AgNPs), 100% cell viability was detected by the cell cytotoxicity assays (both MTT and LDH) at longer times of treatment. This phenomenon may be explained as ‘‘hormesis’’ (Iavicoli et al., 2010). Data gathered from the literature suggest that AgNPs induced hormesis effect is ubiquitous to the organisms since different cell lines, such as HepG2 cells (Jiao et al., 2014), peripheral blood mononuclear cells (Shin et al., 2007), human skin carcinoma cell line A431 and the human fibrosarcoma cell line HT-1080 (Arora et al., 2008) and A549 human epithelial cells (Sthijns et al., 2017), display this behaviour.

Moreover, the fact that in the presence of low NPs/cell amount we observed a decrease in cell viability only at 12 h of incubation time is in accord with our previous results showing autophagy as preferential mechanism induced by low amount of AgNPs-G that occurs, probably, as survival mechanism (Panzarini et al., 2015).

The inverse relationship between the LDH and MTT results further supports the accuracy of our data and corroborate that our synthesis method avoids Ag^+ release. In fact, data in literature show that AgNPs negatively interact with LDH assay *via* enzyme inhibition or binding (Han et al., 2011; Holder and Marr, 2013) or *via* ROS generation (Oh et al., 2014) mediated by Ag^+ presence (Menon and Wright, 1989) that, in turn, affects the accuracy of LDH method for evaluating cytotoxicity.. Moreover, LDH results suggest the presence of necrotic cells upon culture with high amount of AgNPs-G in agreement with data reported in Panzarini et al. (2015).

Loss of cell viability was confirmed by FACS analysis of cell cycle progression during NPs treatment. Data suggest that the presence of higher AgNPs-G amount hampered HeLa cell cycle by arresting cells in S and G2/M phases, decreasing mitotic index and increasing subG1 population, as reported in literature for other cells lines, such as Jurkat T cells (Eom and Choi, 2010) mouse peritoneal Raw 264.7 macrophages (Park et al., 2010), human Chang liver cells (Piao et al., 2011), human lung carcinoma A549 cells (Chairuangkitti et al., 2013), normal human lung IMR-90 fibroblasts and human glioblastoma U251 cells (Asharani et al., 2009), L929 fibroblasts (Wei et al.,

2010) and hepatoma HepG2 cells (Liu et al., 2010). However, our work focused on the study of the effects of AgNPs on cell cycle and not on the mechanism underlying this. On the other hand, the understanding of the mechanisms underlying the perturbation of cell cycle upon AgNPs treatment is still at infancy. The cell cycle is a vital regulator of the cell proliferation and growth process, which protects the cell from DNA damage (Asharani et al., 2009). Literature data concord that the effect of AgNPs on the cell cycle progression mainly depends on the activation of p38 mitogen-activated protein kinase (p38-MAPK), through the oxidative stress nuclear factor-E2-related factor-2 (Nrf-2) and inflammation nuclear factor-kappaB (NF-kB) related transcription factors (Eom and Choi, 2010). In fact, the activation of these signalling pathways induces DNA damage, that in turn gives rise to cell cycle arrest and apoptosis. On the other hand, up regulation of many DNA damage response genes such as Gadd 45 in normal human lung cells, IMR-90 and human brain cancer cells, U251 and ATR in U251 cells (AshaRani et al. 2012) and Bcl-2 and Bax in human breast cancer MCF-7 cells (Baharara et al., 2015) and in human tongue squamous carcinoma SCC-25 cells (Dziedzic et al., 2016) was reported in literature. Moreover, exposure to AgNPs significantly changes the expression levels of selected genes involved in cell cycle regulation. In particular, down regulation of cyclin B1 and E1 and DNA damage response/repair (XRCC1 and 3, FEN1, RAD51C, RPA1) was observed in U251 and IMR-90 cells (AshaRani et al., 2012), in human keratinocytes HaCaT (Bastos et al., 2016) and in human lung epithelial A549 cells (Foldbjerg et al., 2012). In addition, up regulation of cyclin kinase CDK2 (Bastos et al., 2016) and CDK1 (Foldbjerg et al., 2012) was reported.

Finally, it is worth noting highlight that a relation between cell cycle perturbation and uptake of AgNPs is reported (Kim et al., 2011), but it is not yet possible to say whether the perturbation in the cell cycle is due to the internalized NPs or whether the progression of cells through the cell cycle influences the NPs uptake or whether the two processes are sustaining each other.

In conclusion, the use of green method based on the exploiting of β-D-glucose as reducing agent to synthesize AgNPs allowed us to obtain NPs that remained very stable up to 10 days: the glucose

capping was stable and prevented dissolution of NPs and release of Ag^+. AgNPs-G were cytostatic for HeLa cells; once internalized by HeLa cells they blocked cell cycle progression in NPs amount dependent manner. This data suggest that green chemistry synthesized AgNPs-G, could pose the basis for developing new cytostatic therapeutic strategies in cancer therapy. To this aim, further studies are needed; in particular elucidation of the exact mechanism of NPs penetration into HeLa cells and the relationship between cell cycle and uptake must be investigated.

Conflict of interest

The authors declare that there are no conflict of interest.

Acknowledgements

The authors gratefully acknowledge professors D. Manno and A. Serra (University of Salento, Lecce, Italy) for providing AgNPs-G.

References

Ahamed, M., Karns, M., Goodson, M., Rowe, J., Hussain, S.M., Schlager, J.J., Hong, Y., 2008. DNA damage response to different surface chemistry of silver nanoparticles in mammalian cells. Toxicol. Appl. Pharmacol. 233, 404-410.

Albanese, A., Tang, P.S., Chan, W.C., 2012. The effect of nanoparticle size, shape, and surface chemistry on biological systems. Annu. Rev. Biomed. Eng. 14, 1-16.

Arora, S., Jain, J., Rajwade, J.M., Paknikar, K.M., 2008. Cellular responses induced by silver nanoparticles: In vitro studies. Toxicol. Lett. 173, 93-100.

Asharani, P., Sethu, S., Lim, H.K., Balaji, G., Valiyaveettil, S., Hande, M.P., 2012. Differential regulation of intracellular factors mediating cell cycle, DNA repair and inflammation following exposure to silver nanoparticles in human cells. Genome Integr. 3(1), 2.

Asharani, P.V., Hande, M.P., Valiyaveettil, S., 2009. Anti-proliferative activity of silver nanoparticles. BMC Cell. Biol. 10, 65.

Baharara, J., Namvar, F., Ramezani, T., Mousavi, M., Mohamad, R., 2015. Silver nanoparticles biosynthesized using Achillea biebersteinii flower extract: apoptosis induction in MCF-7 cells via caspase activation and regulation of Bax and Bcl-2 gene expression. Molecules 20, 2693-2706.

Bastos, V., Ferreira de Oliveira, J.M., Brown, D., Jonhston, H., Malheiro, E., Daniel-da-Silva, A.L., Duarte, I.F., Santos, C., Oliveira, H., 2016. The influence of Citrate or PEG coating on silver nanoparticle toxicity to a human keratinocyte cell line. Toxicol. Lett. 249, 29-41.

Beer, C., Foldbjerg, R., Hayashi, Y., Sutherland, D.S., Autrup, H., 2012. Toxicity of silver nanoparticles - nanoparticle or silver ion?. Toxicol. Lett. 208, 286-292.

Chairuangkitti, P., Lawanprasert, S., Roytrakul, S., Aueviriyavit, S., Phummiratch, D., Kulthong, K., Chanvorachote, P., Maniratanachote, R., 2013. Silver nanoparticles induce toxicity in A549 cells via ROS-dependent and ROS-independent pathways. Toxicol. In Vitro. 27, 330-338.

Chen, X., Schluesener, H.J., 2008. Nanosilver: a nanoproduct in medical application. Toxicol. Lett. 176, 1-12.

Chiodo, F., Marradi, M., Calvo, J., Yuste, E., Penadés, S., 2014. Glycosystems in nanotechnology: Gold glyconanoparticles as carrier for anti-HIV prodrugs. Beilstein J. Org. Chem. 10, 1339-1346.

Cho, E.C., Au, L., Zhang, Q., Xia, Y., 2010 The effects of size, shape, and surface functional group of gold nanostructures on their adsorption and internalization by cells. Small. 6, 517-522.

Colvin, V.L., 2003. The potential environmental impact of engineered nanomaterials. Nat. Biotechnol. 21, 1160-1170.

Dini, L., Panzarini, E., Serra, A., Buccolieri, A., Manno, D., 2011. Synthesis and in vitro cytotoxicity of glycans-capped silver nanoparticles. Nanomat. Nanotechnol. 1, 58-63.

Dziedzic, A., Kubina, R., Bułdak, R.J., Skonieczna, M., Cholewa, K., 2016. Silver Nanoparticles Exhibit the Dose-Dependent Anti-Proliferative Effect against Human Squamous Carcinoma Cells Attenuated in the Presence of Berberine. Molecules 21, 365.

El-Hussein, A., Mfouo-Tynga, I., Abdel-Harith, M., Abrahamse, H., 2015. Comparative study between the photodynamic ability of gold and silver nanoparticles in mediating cell death in breast and lung cancer cell lines. J. Photochem. Photobiol. B. 153, 67-75.

Eom, H.J., Choi, J. p38 MAPK activation, DNA damage, cell cycle arrest and apoptosis as mechanisms of toxicity of silver nanoparticles in Jurkat T cells. Environ. Sci. Technol. 44, 8337-8342.

Etheridge, M.L., Campbell, S.A., Erdman, A.G., Haynes, C.L., Wolf, S.M., McCullough, J., 2013. The big picture on nanomedicine: the state of investigational and approved nanomedicine products. Nanomedicine. 9, 1-14.

Farr, T.D., Lai, C.H., Grünstein, D., Orts-Gil, G., Wang, C.C., Boehm-Sturm, P., Seeberger, P.H., Harms, C., 2014. Imaging early endothelial inflammation following stroke by core shell silica superparamagnetic glyconanoparticles that target selectin. Nano Lett. 14, 2130-2134.

Foldbjerg, R., Irving, E.S., Hayashi, Y., Sutherland, D.S., Thorsen, K., Autrup, H., Beer, C., 2012. Global gene expression profiling of human lung epithelial cells after exposure to nanosilver. Toxicol. Sci. 130, 145-157.

Goto, H., Tomono, Y., Ajiro, K., Kosako, H., Fujita, M., Sakurai, M., Okawa, K., Iwamatsu, A., Okigaki, T., Takahashi, T., Inagaki, M., 1999. Identification of a novel phosphorylation site on histone H3 coupled with mitotic chromosome condensation. J. Biol. Chem. 274, 25543-25549.

Han, X., Gelein, R., Corson, N., Wade-Mercer, P., Jiang, J., Biswas, P., Finkelstein, J.N., Elder, A., Oberdörster, G., 2011. Validation of an LDH assay for assessing nanoparticle toxicity. Toxicology. 287, 99-104.

Holder, A.L., Marr, L.C., 2013. Toxicity of silver nanoparticles at the air-liquid interface. Biomed. Res. Int. 2013,328934.

Hussain, S.M., Hess, K.L., Gearhart, J.M., Geiss, K.T., Schlager, J.J., 2005. In vitro toxicity of nanoparticles in BRL 3A rat liver cells. Toxicol. In Vitro. 19, 975-983.

Iavicoli, I., Calabrese, E.J., Nascarella, M.A., 2010).Exposure to nanoparticles and hormesis. Dose Response 8, 501-517.

Jiao, Z.H., Li, M., Feng, Y.X., Shi, J.C., Zhang, J., Shao, B., 2014. Hormesis effects of silver nanoparticles at non-cytotoxic doses to human hepatoma cells. PLoS One 9, e102564.

Kennedy, D.C., Orts-Gil, G., Lai, C.H., Müller, L., Haase, A., Luch, A., Seeberger, P.H., 2014. Carbohydrate functionalization of silver nanoparticles modulates cytotoxicity and cellular uptake. J Nanobiotechnology. 12, 59.

Kim, J.A., Åberg, C., Salvati, A., Dawson, K.A., 2011. Role of cell cycle on the cellular uptake and dilution of nanoparticles in a cell population. Nat. Nanotechnol. 7, 62-68.

Kim, S., Ryu, D.Y., 2013. Silver nanoparticle-induced oxidative stress, genotoxicity and apoptosis in cultured cells and animal tissues. J. Appl. Toxicol. 33, 78-89.

Liu, J., Hurt, R.H., 2010. Ion release kinetics and particle persistence in aqueous nano-silver colloids. Environ. Sci. Technol. 44, 2169-2175.

Liu, W., Wu, Y., Wang, C., Li, H.C., Wang, T., Liao, C.Y., Cui, L., Zhou, Q.F., Yan, B., Jiang, G.B., 2010. Impact of silver nanoparticles on human cells: effect of particle size. Nanotoxicology. 4, 319-330.

Loza, K., Diendorf, J., Sengstock, C., Ruiz-Gonzalez, L., Gonzalez-Calbet, J.M., Vallet-Regi, M., Köller, M., Epple, M., 2014. The dissolution and biological effects of silver nanoparticles in biological media. J. Mater. Chem. B. 2, 1634-1643.

Marradi, M., Chiodo, F., García, I., Penadés, S., 2013. Glyconanoparticles as multifunctional and multimodal carbohydrate systems. Chem. Soc. Rev. 42, 4728-4745.

Menon, M.P., Wright, C.E., 1989. A radiotracer probe to study metal interaction with human lactate dehydrogenase isoenzymes. J. Protein Chem. 8, 757-766.

Oh, S.J., Kim, H., Liu, Y., Han, H.K., Kwon, K., Chang, K.H., Park, K., Kim, Y., Shim, K., An, S.S., Lee, M.Y., 2014. Incompatibility of silver nanoparticles with lactate dehydrogenase leakage

assay for cellular viability test is attributed to protein binding and reactive oxygen species generation. Toxicol. Lett. 225, 422-432.

Panzarini, E., Mariano, S., Dini, L., 2015. Glycans coated silver nanoparticles induces autophagy and necrosis in HeLa cells. NANOFORUM 2014, AIP Conf Proc 2015;1667:020017-1–020017-8.

Park, E.J., Yi, J., Kim, Y., Choi, K., Park, K., 2010. Silver nanoparticles induce cytotoxicity by a Trojan-horse type mechanism. Toxicol. In Vitro. 24, 872-878.

Piao, M.J., Kang, K.A., Lee, I.K., Kim, H.S., Kim, S., Choi, J.Y., Choi, J., Hyun, J.W., 2011. Silver nanoparticles induce oxidative cell damage in human liver cells through inhibition of reduced glutathione and induction of mitochondria-involved apoptosis. Toxicol. Lett. 201, 92-100.

Sahay, G., Alakhova, D.Y., Kabanov, A.V., 2010. Endocytosis of nanomedicines. J. Control Release. 145, 182-195.

Sharma, H., Mishra, P.K., Talegaonkar, S., Vaidya, B., 2015. Metal nanoparticles: a theranostic nanotool against cancer. Drug Discov. Today. 20, 1143-1151.

Shin, S.H., Ye, M.K., Kim, H.S., Kang, H.S., 2007. The effects of nano-silver on the proliferation and cytokine expression by peripheral blood mononuclear cells. Int. Immunopharmacol. 7, 1813-1818.

Sthijns, M.M., Thongkam, W., Albrecht, C., Hellack, B., Bast, A., Haenen, G.R., Schins, R.P., 2017. Silver nanoparticles induce hormesis in A549 human epithelial cells. Toxicol. In Vitro 40, 223-233.

Vergallo, C., Panzarini, E., Carata, E., Amhadi, M., Mariano, S., Tenuzzo, B.A., Dini, L., 2016. Cytotoxicity of β-D-glucose/sucrose-coated silver nanoparticles depends on cell type, nanoparticles concentration and time of incubation. NANOITALY 2015, AIP Conf Proc 2016. 1749, 020012-1-020012-9.

Vergallo, C., Panzarini, E., Izzo, D., Carata, E., Mariano, S., Buccolieri, A., Serra, A., Manno, D., Dini, L., 2014. Cytotoxicity of β-D-glucose coated silver nanoparticles on human lymphocytes. NANOFORUM 2013, AIP Conf Proc 2014. 1603, 78-85.

Wei, L., Tang, J., Zhang, Z., Chen, Y., Zhou, G., Xi, T., 2010. Investigation of the cytotoxicity mechanism of silver nanoparticles in vitro. Biomed. Mater. 5, 044103.

Woodrow Wilson Database, 2011. An inventory of nanotechnology-based consumer products currently on the market. http://www.nanotechproject.org/inventories/consumer/analysis_draft/

Zhang, C., Wan, X., Zheng, X., Shao, X., Liu, Q., Zhang, Q., Qian, Y., 2014. Dual-functional nanoparticles targeting amyloid plaques in the brains of Alzheimer's disease mice. Biomaterials. 35, 456-465.

Figure legends

Figure 1. Stability and cristallinity of freshly-prepared and 10-days-old AgNPs-G. a) UV-visible spectra of AgNPs-G/ml in EMEM culture medium reported as absorbance in arbitrary unit (a.u., y axis) *vs* wavelength (nm, x axis). b) TEM diffraction patterns of individual freshly-prepared and 10-days-old AgNPs-G.

Figure 2. Size distribution and shape of freshly-prepared (a) and 10-days-old (b) AgNPs-G. Size distribution is reported as arbitrary unit (a.u., y axis) *vs* longitudinal diameter (nm, x axis). Nanorods are indicated by black arrowheads. bars = 30 nm.

Figure 3. Time course of viability of HeLa cells incubated with AgNPs-G, Ag^+ or β-D-glucose.

A: MTT assay. The viability measured as indicated in Materials and Methods represents the values as percentage of the respective control (untreated cells) ones from three independent experiments considered as 100%. Asterisks indicate significant values ($p<0.05$) from the respective untreated control cells. Ctrl (control) = untreated cells; h = hours.

B: LDH assay. The values are reported as absorbance (mean ± SD from 3 independent experiments) in arbitrary unit (a.u., y axis). Asterisks indicate significant values ($p<0.05$) from the respective untreated control cells. Ctrl (control) = untreated cells; h = hours.

C: LM micrographs show HeLa cells in culture. a) untreated HeLa cells (100% of viability); b) HeLa cells cultured with $2x10^3$ AgNPs-G for 12 hours (-45% of cell viability respect the untreated

cells); c) HeLa cells cultured with $2x10^4$ AgNPs-G for 12 hours (-75% of cell viability respect the untreated cells). bars = 10 μm.

Figure 4. Uptake of AgNPs-G by HeLa cells. A) GF-AAS analysis of the amount of AgNPs-G inside the cells calculated as ppm of silver (mean ± SD from 3 independent experiments) adsorbed by the cells from the culture medium. HeLa cells were treated with different amount of AgNPs-G for different times (t). Asterisks indicate significant value (from the respective untreated control cells ($p<0.05$).

B) ICP-OES analysis of the amount of AgNPs internalized by HeLa cells with different amount of AgNPs-G for different times (t) reported as ratio between the Ag^+ detected in cell extract and those detected in culture medium (absorbance in arbitrary unit, a.u.) from 3 independent experiments.

C) SEM-EDX analysis. SEM images (left upper panel = bright field; right upper panel= dark field) of a representative HeLa cell treated with $2x10^4$AgNPs-G for 2 h and elemental X-ray spectrum (lower panel) of the red square area (right upper panel) containing the white spot. Arrows show AgNPs-G not yet aggregated and still at the cell periphery.

Figure 5. FACS analysis of the effect of AgNPs-G exposure on cell cycle phases. The values measured as indicated in Materials and Methods represents the values as percentage (%) of the respective control (untreated cells) ones from three independent experiments, and report the number of HeLa cells in G0/G1, S and G2/M phases. HeLa cells were treated with different amount of AgNPs-G for 6 (A), 12 (B), 18 (C) and 24 (D) h. Asterisks indicate significant value ($p<0.05$) *vs* untreated cells. Ctrl = untreated cells

Figure 6. Effect of AgNPs-G exposure on the proportion of HeLa cells in the sub-G1 population. HeLa cells were treated with different amount of AgNPs-G for different times. The sub-G1 population size was determined by FACS analysis. All values $2x10^4$AgNPs-G/cell are significantly ($p<0.05$) different respect control (untreated cells); values $2x10^3$AgNPs-G/cell 1 and 18 h are significantly ($p<0.05$) different respect corresponding control without AgNPs-G. Ctrl (control) =

untreated cells; h = hours. Flow cytograms refers to the histogram above. The changes of sub-G1 population are indicated as increased (+) percentages with respect to control at the same time.

Figure 7. Effect of AgNPs-G exposure on Mitotic Index (MI) reported as percentage (%). The fraction of mitotic cells was determined by counting positive HeLa cells irrespective of mitosis phase. At least 500 cells were scored for each time point using a fluorescence microscope. Asterisks indicate significant values ($p<0.05$) respect ctrl (untreated cells). Ctrl = untreated cells. Fluorescence micrographs report representative images of the different phases of mitosis. bar = 10 μm.

Supplementary material

Supplementary figure 1. Kinetic of Ag^+ dissolution. The dissolution of AgNPs-G in complete EMEM culture medium was evaluated by atomic absorption spectroscopy. Each value represents the mean ± SD of three independent experiments, each done in duplicate. Ag^+ dissolution degree is expressed as percentage (%) of total $AgNO_3$ used to obtain the NPs amounts during treatment.

Supplementary figure 2. Representative FACS cytograms obtained with FACScan BD (Becton Dickinson Biosciences, New Jersey, USA) of the cell cycle of HeLa cells cultured with different amounts (2x103 and 2x104) of AgNPs-G/cell for different times (6, 12, 18 and 24 h).

Figure 1

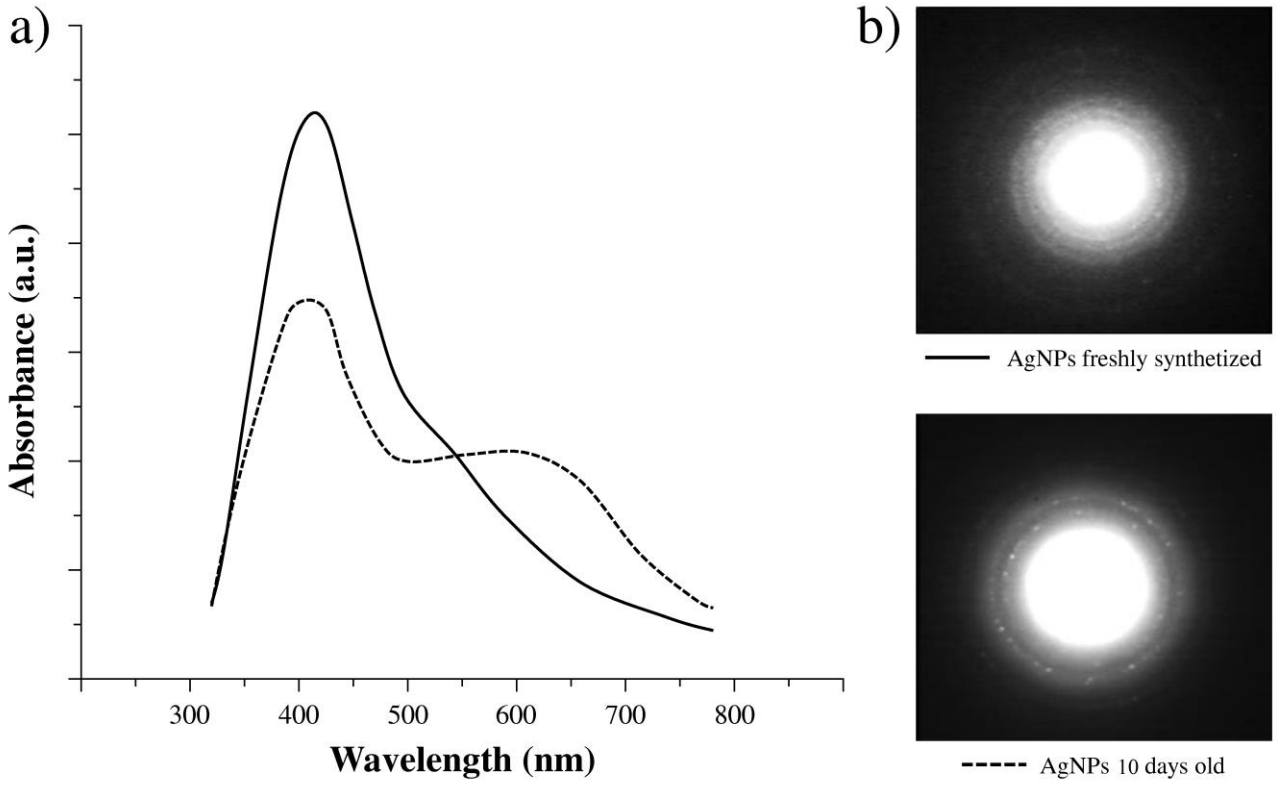
a)
Absorbance (a.u.)
300
400
500
600
700
800
Wavelength (nm)
b)
AgNPs freshly synthetized
AgNPs 10 days old

Figure 2

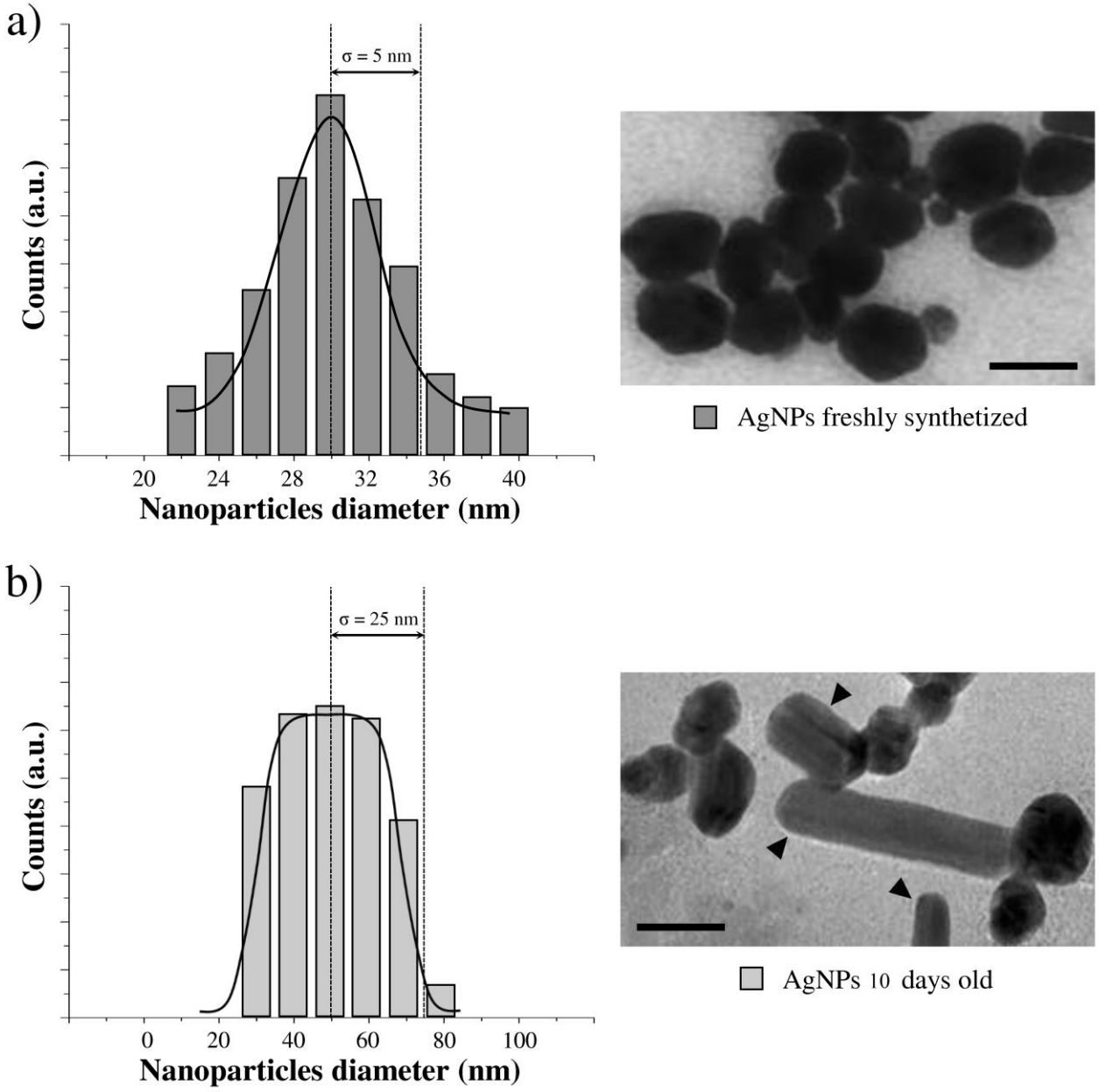
a)
σ = 5 nm
Counts (a.u.)
20
24
28
32
36
40
Nanoparticles diameter (nm)
AgNPs freshly synthetized
b)
σ = 25 nm
Counts (a.u.)
0
20
40
60
80
100
Nanoparticles diameter (nm)
AgNPs 10 days old

Figure 3

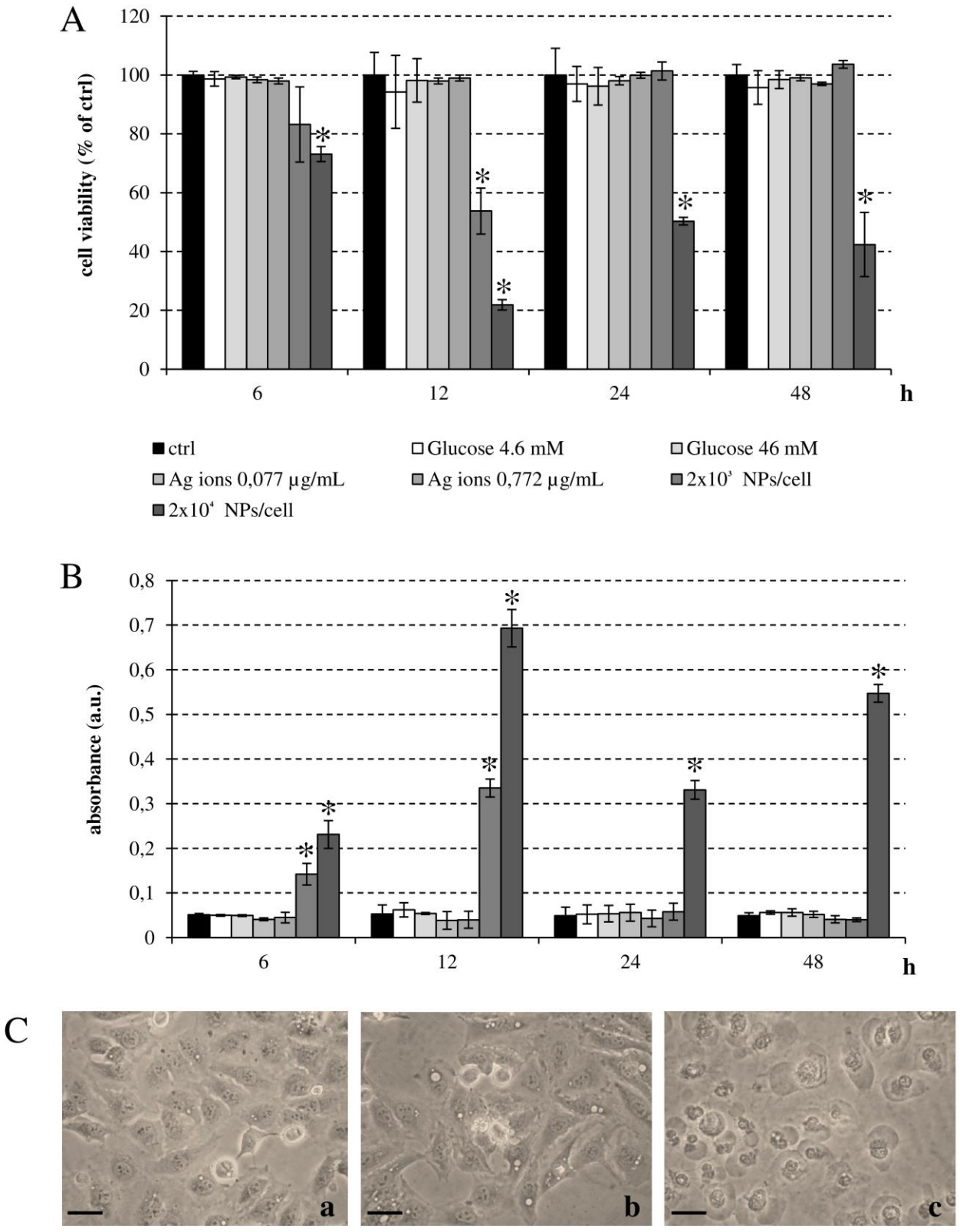
A
cell viability (% of ctrl)
120
100
80
60
40
20
0
6
12
24
48
h
ctrl
Glucose 4.6 mM
Glucose 46 mM
Ag ions 0,077 µg/mL
Ag ions 0,772 µg/mL
2x10³ NPs/cell
2x10⁴ NPs/cell
B
absorbance (a.u.)
0,8
0,7
0,6
0,5
0,4
0,3
0,2
0,1
0
6
12
24
48
h
C
a
b
c

Figure 4

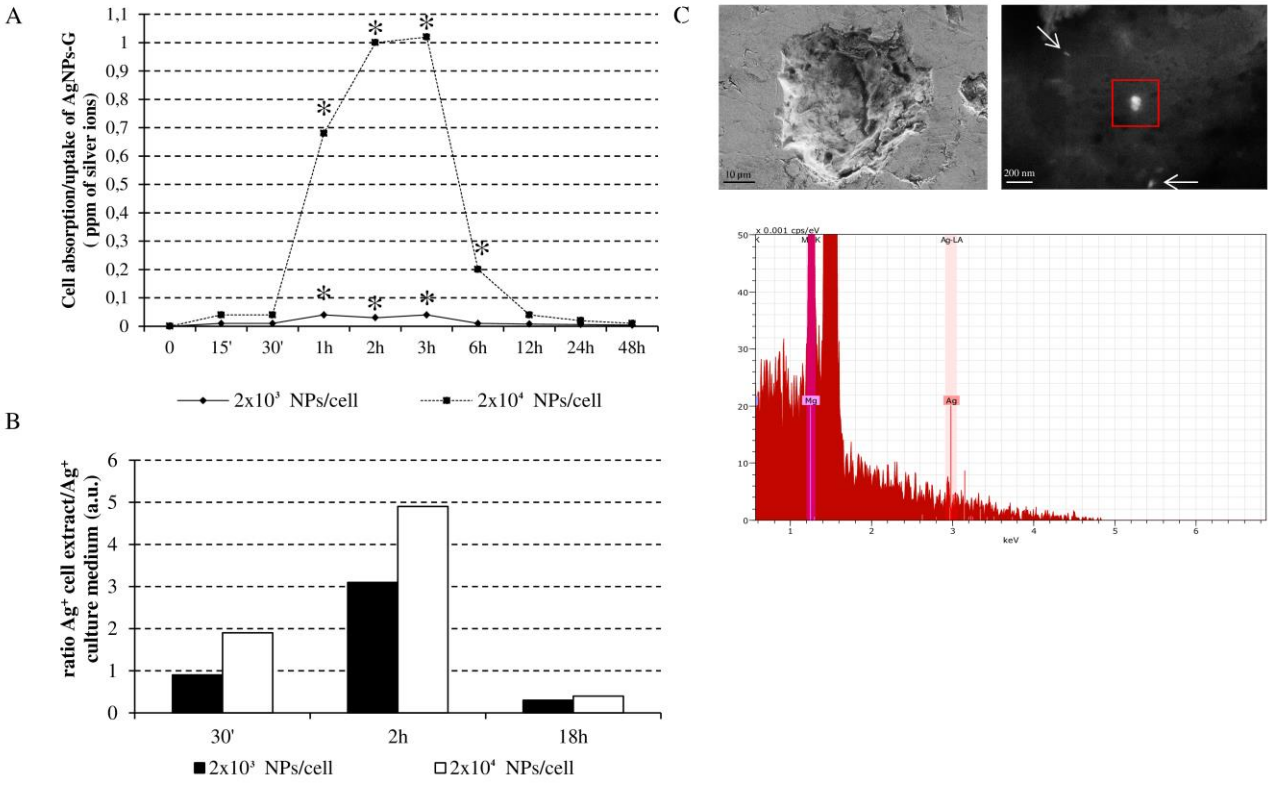
A
Cell absorption/uptake of AgNPs-G
(ppm of silver ions)
1,1
1
0,9
0,8
0,7
0,6
0,5
0,4
0,3
0,2
0,1
0
0
15'
30'
1h
2h
3h
6h
12h
24h
48h
2x10³ NPs/cell
2x10⁴ NPs/cell
B
ratio Ag⁺ cell extract/Ag⁺
culture medium (a.u.)
6
5
4
3
2
1
0
30'
2h
18h
2x10³ NPs/cell
2x10⁴ NPs/cell
C
10 µm
200 nm
x 0.001 cps/eV
Mg-K
Ag-LA
Mg
Ag
50
40
30
20
10
0
1
2
3
4
5
6
keV

Figure 5

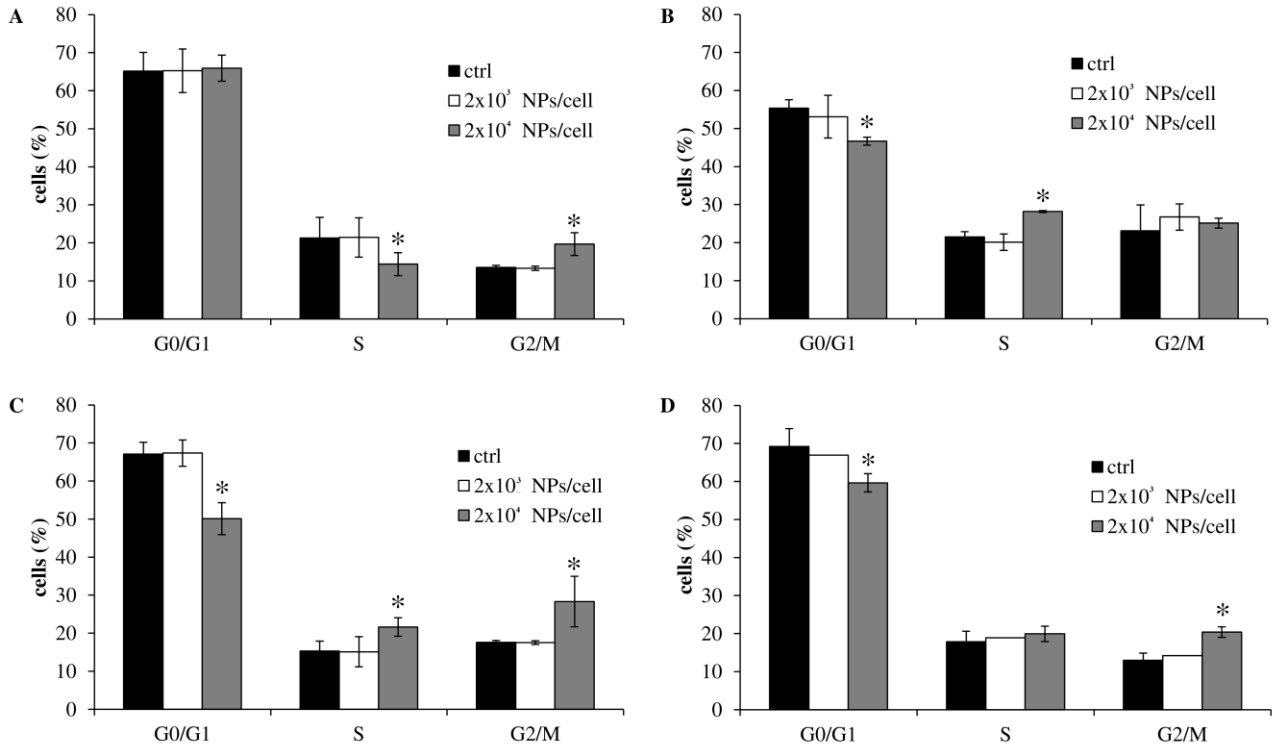
A
B
C
D
cells (%)
ctrl
2x10³ NPs/cell
2x10⁴ NPs/cell
G0/G1
S
G2/M
0
10
20
30
40
50
60
70
80
*

Figure 6

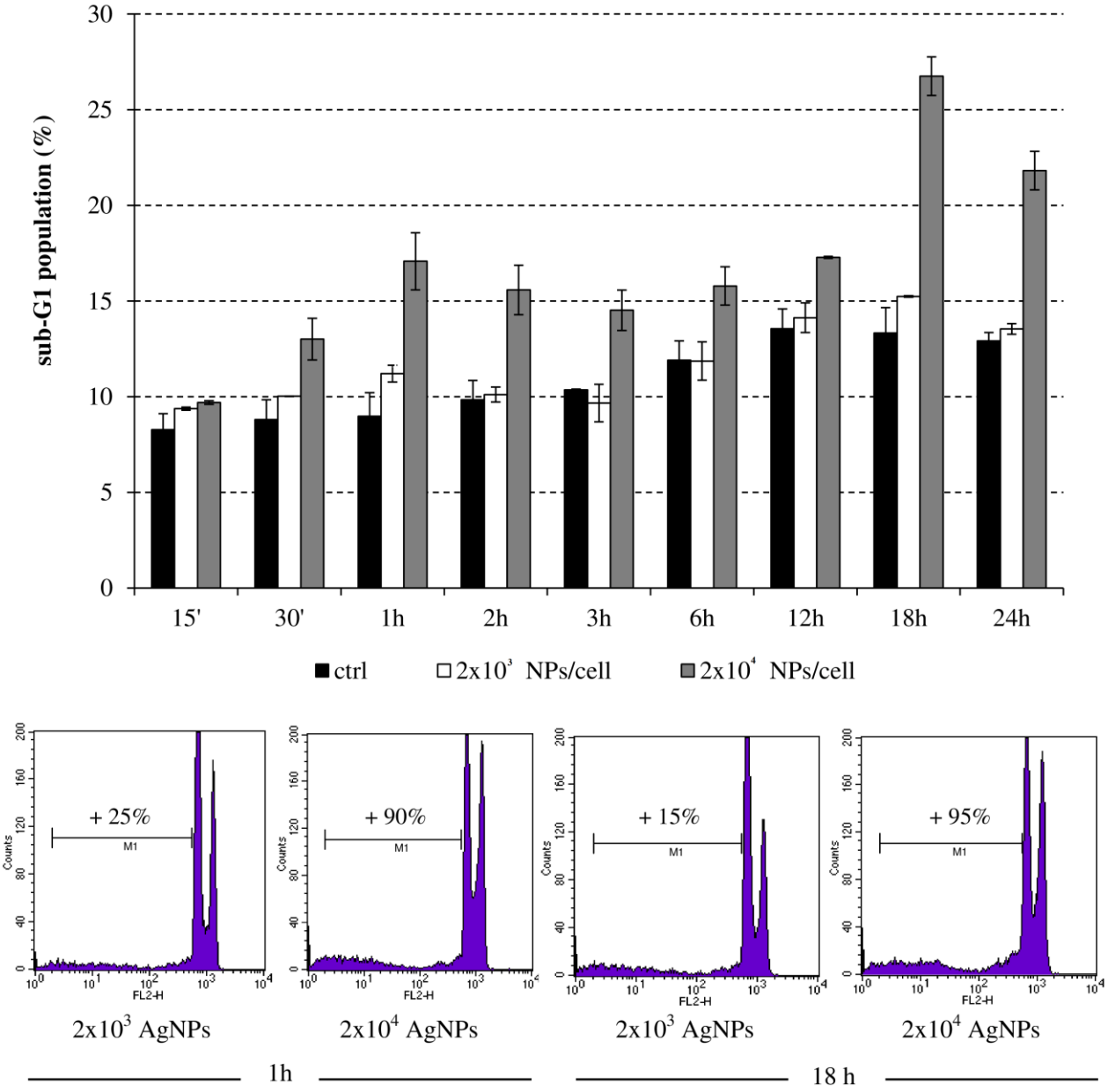
sub-G1 population (%)
30
25
20
15
10
5
0
15'
30'
1h
2h
3h
6h
12h
18h
24h
ctrl
2x10³ NPs/cell
2x10⁴ NPs/cell
+ 25%
+ 90%
+ 15%
+ 95%
M1
Counts
FL2-H
2x10³ AgNPs
2x10⁴ AgNPs
2x10³ AgNPs
2x10⁴ AgNPs
1h
18 h

Figure 7

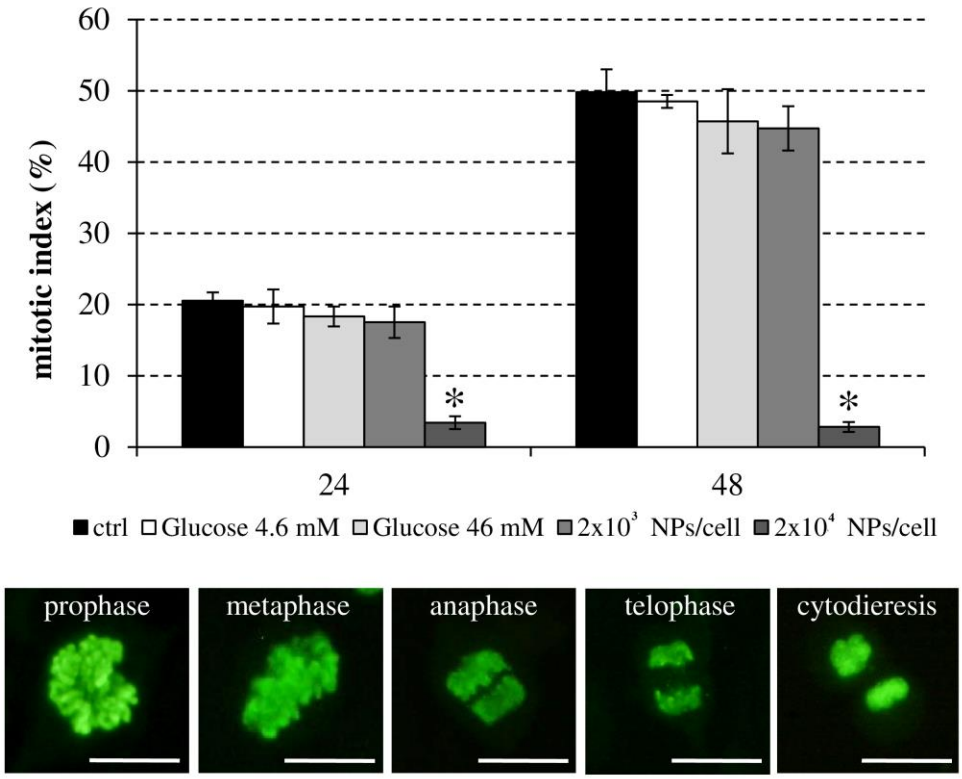
60
50
40
30
20
10
0
mitotic index (%)
*
*
24
48
ctrl
Glucose 4.6 mM
Glucose 46 mM
2x10³ NPs/cell
2x10⁴ NPs/cell
prophase
metaphase
anaphase
telophase
cytodieresis

Graphical abstract

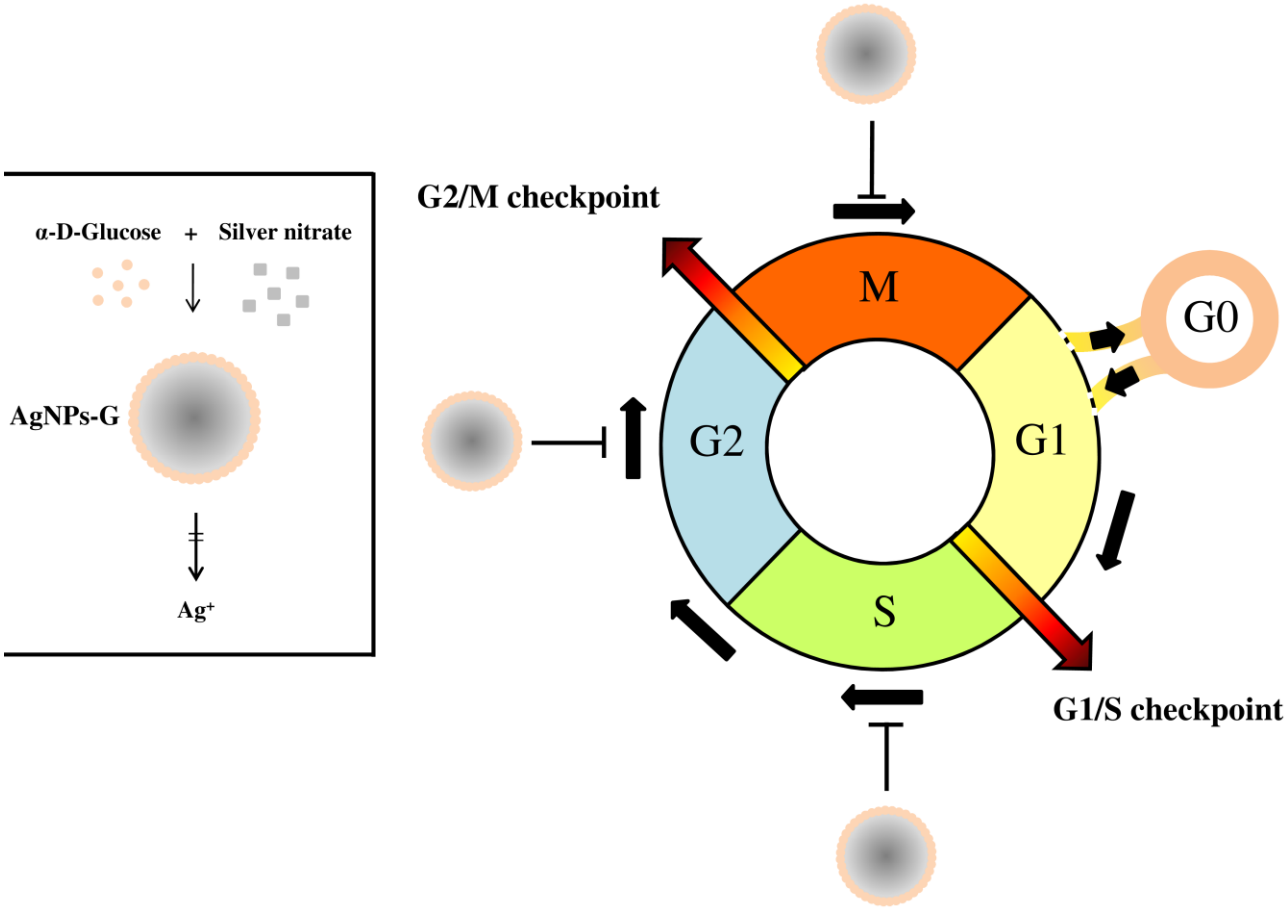

Supplementary Figure 1

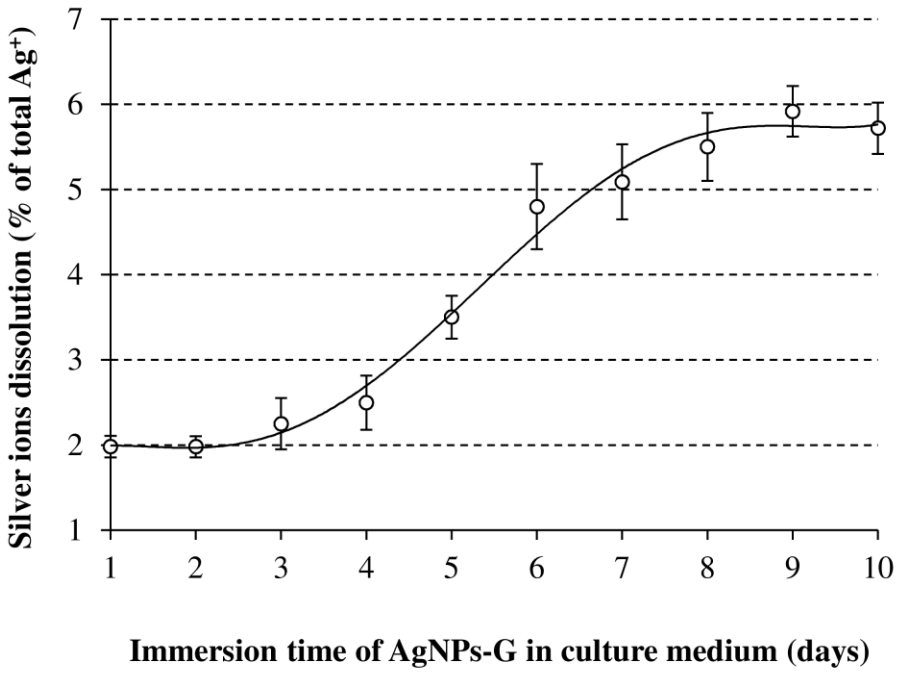

Supplementary Figure 2

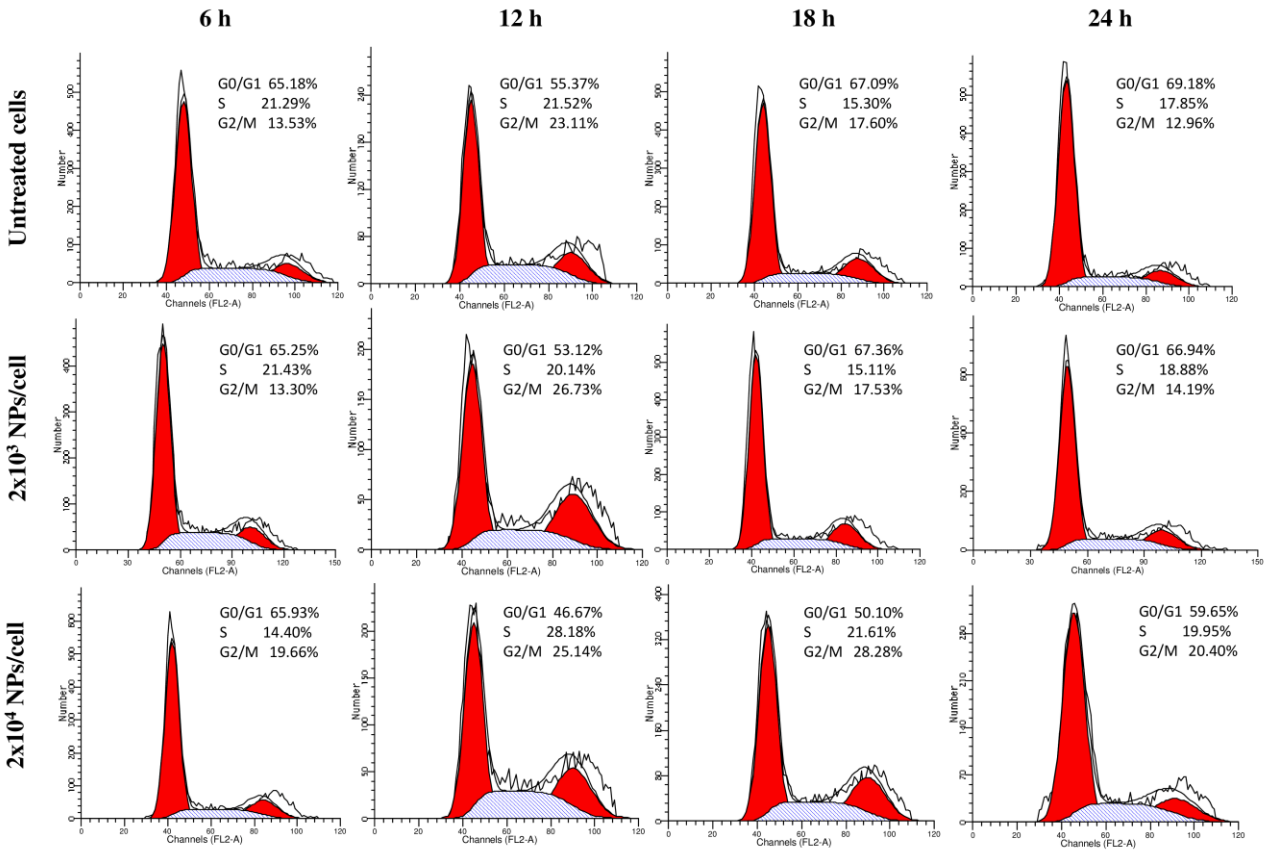

Table 1. Dissolution on AgNPs-G in complete EMEM culture medium

Immersion time (days)	Silver concentration (µg/mL)		Degree of dissolution (%)
	2×10^3 NPs/cell	2×10^4 NPs/cell	
1	0,026	0,267	1,98
2	0,026	0,267	1,98
3	0,030	0,303	2,25
4	0,034	0,337	2,49
5	0,047	0,472	3,50
6	0,065	0,648	4,79
7	0,069	0,687	5,09
8	0,074	0,742	5,50
9	0,079	0,798	5,91
10	0,077	0,772	5,72

Dissolution experiment up to 10 days performed in complete EMEM culture medium of AgNPs-G solutions corresponding to amounts used to reach 2×10^3 NPs/cell and 2×10^4 NPs/cell during experiments of cytotoxicity, uptake and cell cycle perturbation. The dissolution of AgNPs-G, in terms of release of Ag+, was determined by atomic absorption spectroscopy as reported in Methods section. Results were expressed as the mean amount of Ag in µg/mL. Ag^+ dissolution degree is expressed as percentage (%) of total AgNO3 used to obtain the NPs amounts during treatment.